

Article

Identifying Economic and Clean Strategies to Provide Electricity in Remote Rural Areas: Main-Grid Extension vs. Distributed Electricity Generation

Bandar Jubran Alqahtani  and Dalia Patino-Echeverri *

Nicholas School of the Environment, Duke University, Durham, NC 27708, USA

* Correspondence: dalia.patino@duke.edu

Abstract: The policy decision of extending electric power transmission lines to connect a remote area to a primary grid vs. developing local electricity generation resources must be informed by studies considering both alternatives' economic and environmental outcomes. Such analysis must also consider the uncertainty of several factors such as fuel prices, the cost and performance of renewable and conventional power generation technologies, and the value of environmental benefits. This paper presents a method for this analysis, making two main contributions to the literature. First, it shows how to characterize the two alternatives (i.e., main-grid extension vs. local power generation) in detail for precise quantification of their capital and operating costs while guaranteeing that they are both adequate to meet forecast demand and operating reserves. Second, it shows how to properly account for the economic and environmental implications of renewable energy intermittency and uncertainty through the optimization of capital investments and hourly operations. The method is illustrated by applying this analysis method to Saudi Arabia, where the government is struggling to outline a strategy to meet residential and commercial loads reliably and sustainably in the country's remote, scattered, isolated areas. To meet this demand, the Saudi government is considering two main alternatives: (1) extending the primary power transmission grid; or (2) installing an optimal combination of off-grid distributed generation (DG) resources, including solar PV, wind, diesel, oil, heavy fuel oil, and Li-ion batteries, to generate the electricity locally. Results suggest that under most scenarios of capital costs, fuel prices, and costs of air pollution, developing a microgrid with a large share of wind and solar power is more cost-effective than extending a primary grid 150 km or more away. Extending a primary grid powered by gas-fired combined-cycle power plants is more economical only if the load is not very high, the distance is not more than 350 km, and oil prices are relatively high compared to natural gas.

Keywords: renewable; energy access; distributed generation; microgrid; emissions; capacity expansion planning; rural electricity; solar PV; wind power; batteries



Citation: Alqahtani, B.J.; Patino-Echeverri, D. Identifying Economic and Clean Strategies to Provide Electricity in Remote Rural Areas: Main-Grid Extension vs. Distributed Electricity Generation. *Energies* **2023**, *16*, 958. <https://doi.org/10.3390/en16020958>

Academic Editor: Rajendra Singh Adhikari

Received: 30 November 2022

Revised: 27 December 2022

Accepted: 10 January 2023

Published: 14 January 2023



Copyright: © 2023 by the authors. Licensee MDPI, Basel, Switzerland. This article is an open access article distributed under the terms and conditions of the Creative Commons Attribution (CC BY) license (<https://creativecommons.org/licenses/by/4.0/>).

1. Introduction

Despite encouraging progress in electricity access and sustainability, in 2019, there were 759 million people without this vital service [1]. Most unserved communities are in rural areas, distant from urban centers and the electric power grid. When evaluating a strategy to increase electricity access, a critical question is whether extending the primary grid is preferable over developing infrastructure to generate electricity locally with fossil fuels (such as diesel) or renewables (biomass, wind, solar, or mini-hydro). Responding to this question requires analysis that considers in detail the operations of the different generators to guarantee reliable supply and the associated economic and environmental outcomes.

This paper presents a method for a thorough techno-economic assessment of the electricity supply options available to reliably and sustainably meet residential and commercial

loads located in remote, scattered, isolated areas. We illustrate the analysis with a case study of Saudi Arabia over the 2024–2040 planning horizon. The study aims to determine whether off-grid DG is a more cost-effective and environmentally sustainable alternative to extending the primary national grid to interconnect significant isolated loads.

The method proposed in this paper differs from previous studies in that it adequately sizes all the components of the two alternatives to supply the electricity demand in remote areas and hence more precisely estimates their associated costs. The method accomplishes this through the consideration of hourly data. This high temporal resolution allows representation of the daily and seasonal variability in solar and wind resources and the operating constraints of all generation and transmission resources to guarantee resource adequacy. Ensuring resource adequacy means that when the two alternatives—main-grid extension vs. off-grid distributed generation—are compared, they both have adequate capacity to meet the load and maintain operating reserves.

Some prior studies published in the literature have attempted to compare the economics of the main-grid-extension option with off-grid DG. Thushara et al. [2] developed a multi-criteria decision analysis model to determine the best choice for supplying electricity to Sri Lanka as an isolated island, including alternatives of interconnecting to neighboring countries' grids and installing central power generation technologies. Similarly, Trotter et al. [3] and Moretti et al. [4] developed long-term multi-objective capacity planning models to supply electricity optimally in Uganda and the Sub-Saharan, considering a combination of off-grid and grid-extension options. More recently, Nock et al. [5] formulated a generation-expansion planning problem to find an optimal mix of centralized and distributed resources that maximizes social benefit. While they make a significant contribution, these optimization models often characterize the supply alternatives by looking at their projected annual production, costs, and emissions but ignore technical constraints and associated challenges in procuring required ancillary services necessary to integrate variable renewable energy resources.

Other prior studies compare the leveled costs of different DG alternatives with the grid-extension option. Some approaches do not use an optimization model [6,7], while some use HOMER [8,9], a simplified LP model [10,11], or a minimum spanning tree (MST) algorithm model [12]. While these studies are also helpful, they ignore the inter-hourly energy fluctuations from off-grid variable renewable energy and their effect on ancillary services requirements. Some of these studies may also fail to properly account for the increased costs of grid extension. Supplementary S4 provides more details on the scope and findings of these studies.

The main contributions of this paper to the existing literature are: (a) the precise estimation of a grid extension's cost; and (b) the precise estimation of the costs of the off-grid system through its optimal configuration and consideration of the inter-hour fluctuations of energy from wind and solar resources. This study conducts a power flow analysis for the main-grid-extension option (MGE) to determine the specifications of required systems components such as transmission lines, shunt reactors, transformers, etc. It then calculates the total cost of grid extension to be compared with the optimal off-grid DG (microgrid) option. In addition, the optimal energy mix of the distributed generation is determined based on hourly operations and performance of the DG technologies instead of monthly or yearly outputs, so it precisely addresses the inter-hour power output fluctuation and intermittency of renewable energy resources. Finally, this study analyzes how uncertainty about future fuel prices, emissions costs, and renewable energy technologies costs might affect the optimal choice. The method followed in this analysis can inform electricity system capacity planning in other rural regions of the world.

Other contributions of this paper are its findings regarding the economics of power generation with wind, solar, and modern combustion turbines. Results for the three areas considered in the case study indicate that local microgrids adequately sized to meet the load are more cost-effective than extending the grid for a distance longer than 150 km. Wind

power is part of an economically optimal capacity mix, even in areas with unimpressive wind resources and rich solar resources.

2. Materials and Methods

2.1. Methods Overview

The method for comparing the economics of the two alternatives, i.e., grid extension vs. microgrid, consists of determining the size of all the components necessary for each to meet the load reliably and then quantifying their capital and operating costs. Reliability in this context means that the system is “resource-adequate”, so it can meet the load and maintain operating reserves during all the periods considered.

To quantify the costs of the main-grid-extension (MGE) alternative, we first characterize the baseline system, representing its high-voltage buses, power generators, and transmission lines. We then determine the power generation expansion needed to meet the new load from the remote area and the characteristics of the power transmission infrastructure required to interconnect it. We use Siemens’ PSSE—a power system simulation software—to represent this grid with the added power generation capacity and transmission interconnections required to serve the remote areas. The final costs of the MGE alternative include transmission line extensions, transformer and substation installations, and installing and operating all the additional power generation required to meet the load of the remote area.

To quantify the costs of the off-grid alternative, we determine the optimal power generation capacity mix required to meet the local load in the remote areas for each hour of a simulated year. How much capacity to install of each possible power generation technology is determined via optimization with a mixed-integer linear program (MILP) described in Section 2.4. The decision variables are: whether to install different power generation and storage alternatives, including wind, solar, fossil-fuel-fired combustion engines, and Li-ion batteries; and how to operate them hour by hour. The objective is to minimize the capital and operating costs while abiding by several constraints imposed by the technical limits of the generators and by operating rules (such as maintaining adequate operating reserves).

2.2. Case Study

This paper analyzes the strategy used by the Saudi Electric Company (SEC) to meet growing electricity demand in three remote, non-interconnected areas. SEC is mainly owned by the government and Saudi Aramco (81% of SEC shares), and is a monopoly for electricity transmission, distribution, and retail supply. It serves residential, commercial, and industrial customers and manages 65% of the country’s total installed power generation capacity (55.3 GW in 2019) [13,14]. The other major electricity producers in the country are the government-owned Saline Water Conservation Corporation (SWCC) and Jubail Water and Power Company, accounting for 9% and 3%, respectively, of the total generation capacity [15]. The electricity-generating business is open to the private sector, so several privately owned generators (i.e., Independent Power Producers (IPPs)) produce and sell power to SEC or directly supply electricity to isolated loads. However, SEC is the only wholesale buyer from privately owned generators and is responsible for selling the electricity to final consumers [13]. All utilities in Saudi Arabia rely heavily on partially subsidized fossil fuels as feedstock for generating electricity. Crude oil, diesel, and heavy fuel oil (HFO) account for two-thirds of the input for electricity generation, and natural gas provides most of the remaining share [15].

The National Grid SA Company, wholly owned by SEC, is responsible for planning, building, and operating a massive electricity transmission and distribution network that extends to cities, towns, and villages across the country [13,14]. SEC has faced several challenges over the past two decades. Demand and peak load have risen by more than 45% from 2010 to 2019, so SEC has increased its total available capacity by 38% from 40 GW to 55 GW, incurring a massive cost. It has also extended the grid’s length by

84%, from 46,179 km to 84,787 km [14], but more than 20 remote networks/loads remain disconnected [14]. To address demand growth, SEC has developed a plan to increase its available power generating capacity from multiple technologies, including fossil-fuel combined cycle, integrated solar combined cycle (ISCC), solar PV, and wind [14]. Its goal is to generate 9.5 gigawatts from renewable energy by 2023, in line with Saudi Arabia's Vision 2030 [16].

However, SEC sees it necessary to explore more economical and sustainable alternatives to grid extension because of the load's magnitude and growth and the considerable investment required to interconnect them to the primary grid. A combination of off-grid distributed electricity generation technologies (off-grid DG) seems a sensible alternative to investment in grid extension and construction of sizable, centralized power plants. Off-grid DG promises economic and environmental benefits from eliminating transmission and distribution costs, deferring capital costs of large central power plants, reducing greenhouse gas emissions, and improving the availability and reliability of electrical networks.

The following sections describe the case study, analyses' assumptions, and steps followed in conducting a techno-economic evaluation and comparing the main-grid-extension (MGE) with the alternative power generation options.

2.2.1. Assumptions and Data

The scope of the case study is limited to three remote, scattered, isolated networks in different regions of Saudi Arabia. Table 1 summarizes essential information about these areas, which differ in their electricity consumption, distance from the primary grid, and renewable energy resources. The first and largest area is Sharorah, located in the far south next to Yemen. The second and smallest area is about 500 km east of Sharorah. The third area is in the northeastern region close to Iraq, less than 150 km from the primary grid. These areas have experienced rapid growth over the last decade and are currently powered by old and polluting, third-party-owned oil and diesel engines rented to the SEC (see Supplementary S1 for characteristics of these generators).

Table 1. The major isolated areas to be studied.

Isolated Load	Region	Existing System (as of 2020)			Distance from the Grid (Km)	Electricity Demand Annual Growth Rate (2021–2040)
		Capacity (MW)	Peak Load (MW)	Gen. (MWh)		
Kharkhir	Southern	17	14	49,996	503	1.3%
Uwayqilah	N Eastern	28.8	25.1	124,344	145	1.6%
Sharorah	Southern	226	127	624,335	340	2.0%

2.2.2. Main-Grid-Extension (MGE) Costs

Table 2 lists assumptions about generation and transmission lines characteristics and costs (all costs are in 2018 dollars) considered when evaluating the main-grid-extension option (MGE). It is assumed that 90% of the electricity that the primary grid would supply to the newly interconnected loads would be generated by an oil-fired combined cycle power plant similar to the one commissioned in 2015 in the eastern region of KSA [17]. The remaining 10% would be generated by either solar PV or wind, which are expected to be integrated into the primary grid, representing 10% of the installed capacity by 2023 [18,19]. The grid-connected solar PV is assumed to be in the city of Tabouk in the northwestern area of Saudi Arabia. This region has excellent solar resources (its global horizontal irradiance (GHI) is 2308.4 kWh/m²/year) and is expected to house most of the kingdom's future solar PV capacity [18]. The grid-connected wind-power generation is assumed to be in the Waad Alshamal area in the northern region. With the best wind resources in KSA and an average wind speed of 7.46 m/s at 92 m height, it will host the first set of multi-hundred-megawatt wind-generation facilities. See Supplementary S2 for more details on wind and solar resources in these areas.

Table 2. Assumptions on technical characteristics and costs of fossil-fired combined-cycle power plants (CCPPs) and transmission lines.

Parameter	Location		
	Sharorah	Kharkhir	Uwayqilah
T/L length (km)	340	503	145
T/L voltage rating (kV)	380	132	132
T/L cap cost (\$/km) *	450	190	190
Annual T/L O&M cost (% of Capex) *	5	5	5
Substation/Transformer cost (\$k) *	3990	2760	2760
Shunt reactor (\$k/MVar) *	21	21	21
T/L power losses (%) **	8	8	8
Capital costs of centrally dispatched CCPPs to meet new load (\$/MW) ***	788	788	788
Annual non-fuel O&M costs of grid-connected CCPPs (\$/MW) ***	10.3	10.3	10.3
Energy efficiency of CCPPs (%) ***	52	52	52

* Costs were provided by SEC and match estimates by Black & Veatch for the Western Electric Coordinating Council (WECC) [20]. The only exception is the transmission line's capital costs, which are about a third of those in the US, mainly due to differences in labor costs. Costs in 2018 USD. ** The transmission lines' losses are based on average values reported by SEC over the last five years [15]. *** Power plant's capital cost and efficiency are similar to those reported for the latest commissioned combined cycle power plant in Saudi Arabia [17], converted to 2018 USD assuming an inflation rate of 2%. These costs are only 0.7% less than the U.S. Energy Information Administration (EIA) estimate, which is 794 k USD/MW [21]. Annual O&M costs are identical to those estimated by EIA [21].

While the capital costs of the new fossil-fired combustion engines for power generation are assumed to be unchanged during the planning horizon, their operating and maintenance costs will vary every year with the price of fuel. As discussed in Section 2.4, three different scenarios for fossil fuels are considered.

On the other hand, the expected changes in the capital costs of wind and solar power generation result in one having a lower cost of electricity than the other in different years. Considering three scenarios of wind and solar capital costs results in different assumptions about the generation technology that supplies 10% of the load in the primary grid.

2.2.3. Off-Grid Distributed Generation (DG)

Off-Grid Conventional Power Generator Operational Parameters

The isolated areas considered in this study are currently supplied by electricity generated locally with diesel/oil engines rented by the SEC. It is assumed that all the power plants to be retired in 2024 and 2025 will be replaced with combustion turbines similar to the Wärtsilä engine used in many places worldwide, including Saudi Arabia. This technology offers high efficiency of 47–49%, fast ramping capability, and its fuel-flexible engine can run using gas, oil, HFO, and diesel [22]. According to its technical specifications, this engine also has no minimum run time and only requires a minimum downtime of 5 min, allowing an unrestricted number of start-ups and shut-downs per day with no impact on O&M [22]. It has an effective ramp rate of 50% per minute and, when it is preheated, it can be synchronized with the grid in 30 s, reaching maximum output in 3 min [22,23]. Thus, it is assumed that it has zero start-up cost [23] and a minimum continuous stable loading of 30% [22]. Such operational features are used in similar modern reciprocating combustion engines to substitute for new aero-derivative combustion turbines [24]. In addition to the replacements, any acquisitions of fossil-fired electric generating capacity are assumed to be of this technology.

The average heat rate of the new combustion engine is assumed to be equal to that of the recently installed diesel engine in Sharorah, which is 8508 Btu/kWh. The greenhouse

gas emissions rates from burning diesel, oil, or HFO are assumed to be like those reported by the Intergovernmental Panel on Climate Change (IPCC) [25].

Off-Grid PV System Assumptions

The hourly electricity generation from solar PV panels, G_{PV} (W), is estimated using Equation (1), which relates the amount of irradiance hitting the tilted surface of the polycrystalline PV modules, I_m (W/m^2), with the nameplate PV capacity, PV_c (W), adjusted to the efficiency of the polycrystalline PV modules of 17%; a de-rating factor of 77% to account for reductions in power output due to soiling of the modules, inverter losses, wiring losses, module mismatch, etc.; and the effect of module's temperature, T_c ($^{\circ}C$), which is assumed to cause a 0.5% reduction in PV power generation for each degree Celsius of the module's temperature exceeding $25^{\circ}C$ [26,27].

$$G_{PV} = 0.77 \times PV_c \left(\frac{I_m}{1000 \frac{W}{m^2}} \right) \times [1 - 0.005(T_c - 25^{\circ}C)] \quad (1)$$

The module temperature's values, T_c , are estimated for each hour of the year according to [28], using data on ambient temperature, GHI, and wind speed. The values of hourly direct irradiance hitting the tilted module surface are estimated based on the hourly GHI values and the sun's position relative to the tilted module, as in [29]. The PV system is assumed to experience an annual compound rate of efficiency decay of 0.5% as in [26,27]. The hourly data of GHI, ambient temperature, and wind speed for all locations were obtained from Saudi Aramco, based on field measurements made in 2016, and summarized in Table 3. These values are consistent with the monthly average values reported in the NASA Surface meteorology and Solar Energy database over the 2000–2004 period [30].

Table 3. Solar and wind resources and climate conditions in isolated areas observed in 2016.

Parameter	Sharorah	Kharkhir	Uwayqilah
GHI [$kWh/m^2/year$]	2371	2339	2097
Temperature [T°]	25.8	28.2	22.62
Relative Humidity [%]	25.11	25.7	29.31
Ground Wind speed (m/s)	3.2	3.5	3.8
Annual Avg. air density (kg/m^3)	1.0768	1.1123	1.1351
Annual Avg. wind speed at 92 m height (m/s)	6.053	6.284	6.372
Annual Avg. pressure (kPa)	92.573	96.298	96.302
Annual Avg. temperature (K)	299.78	301.93	296.02
Average C_p	0.3568	0.3586	0.3572

Off-Grid Wind Energy Assumptions

The hourly electricity generation from converting wind power into rotational energy in the wind turbine is estimated from Equation (2) [31]:

$$G_{wind} = \frac{1}{2} \times \rho \times A \times v^3 \times C_p = \frac{1.742}{T} \times p \times A \times v^3 \times C_p \quad (2)$$

where

- ρ is air density in kg/m^3 ;
- A is the swept rotor area in m^2 ;
- v is the wind speed in m/s ;
- p is the pressure in kPa ;

T is the temperature in kelvin; and

C_p is the turbine power coefficient. It is unique to each turbine type and is a function of wind speed.

Data on hourly wind speeds and other atmospheric conditions were collected by Saudi Aramco based on field measurements made in 2016 and are summarized in Table 3. This data is consistent with the yearly average values reported in the KA-CARE Renewable Resource Atlas for 2014–2016 [32]. The assumed wind turbine technical specifications are similar to those of a GE 2.75-120 wind turbine [33] installed in 2013 in Turaif in the northwestern area of Saudi Arabia. It is considered the most advanced wind power technology; with a rotor diameter of 120 m and swept rotor area of 10,825 m², it achieves a high-power coefficient with cut-in and cut-out speeds of 3 and 25 m/s, respectively [34] and can be installed at heights of 85–139 m. These characteristics make wind energy more cost-competitive in areas with inadequate wind resources, such as the remote areas under study. So far, there have been at least 20 such installations in five countries in Asia and Europe [34].

Off-Grid Energy Storage

The energy storage system considered in this study is a lithium-ion battery unit with round trip efficiency of 86%, 4% annual performance degradation, ten-year lifetime, charging/discharging duration capacity of 4 h, and 100% of depth of battery discharge (DOD) (i.e., the battery can fully discharge all its energy content) [35,36]. When installed, it would compensate for fluctuations in electricity generation from variable renewable energy and sudden load changes, providing power and spinning reserves.

Costs and Other System Assumptions

There are limited public sources of information on the costs of installing and maintaining modern combustion engines. In this study, we assume the capital and annual fixed costs for diesel-powered engines are 750 K USD/MW and 13.4 K USD/MW, respectively, based on actual quotations close to figures reported by Lazard [37] and much lower than figures reported by EIA, US DOE, AEMO, and E3 [24,37–40]. The oil and HFO-powered engines are assumed to have capital and annual fixed costs that are 10% and 20% higher than diesel engines, consistent with the actual quotation. The weighted average cost of capital (WACC) is assumed to be 7%, with 20 years to maturity and an inflation rate of 2%, based on the values used by the Water & Electricity Regulatory Authority (WERA) (formerly called Electricity Cogeneration Regulatory Authority (ECRA)) to assess new power plant projects, including those for renewable energy [according to personal correspondence with the WERA's vice governor].

Fuel costs for the planning horizon are estimated based on projections from different sources. Oil prices are based on the annual average oil prices presented in the OPEC 2016 world oil outlook, which has been the latest published oil price projection by OPEC; we consider the prices reported for the reference case and the low and high oil price cases [41]. Similarly, as Saudi Arabia consumes all locally produced natural gas and does not exports any, estimates of annual average prices of natural gas corresponding to reference, high, and low oil price scenarios are equal to the projections of Henry Hub Spot Prices presented in the EIA's Annual Energy Outlook 2021 (AEO2021) [42] as suggested by a leading Saudi investment management and advisory firm [43]. The yearly average diesel and HFO prices are calculated relative to oil prices, assuming diesel's prices to be 37% higher than oil prices while HFO prices would be 27% lower than oil prices. This is based on a report of historical EIA monthly refiner petroleum product prices for 2010–2020 [44]. We also account for the costs of transporting fuels to the distributed generation facilities from the nearest node in Aramco's fuel distribution network. A transportation cost of 0.024 USD/km to deliver a barrel of fuel to the generation site [according to personal correspondence with SEC/Planning Department] is added to the generation marginal costs. Although KSA does not currently account for the cost of GHG emissions, this study considers scenarios where

emissions of CO₂, N₂O, and CH₄ are priced at the value estimated by the Interagency Working Group (IWG) on the Social Cost of Greenhouse Gases in the US [45] under 5%, 3%, and 2.5% discount rates.

The projected solar PV and wind's capital and O&M costs over 2024–2040 are based on low, mid, and high values reported by the NREL's 2020 Annual Technology Baseline (ATB) workbook [46]. The projected capital and O&M costs of lithium-ion (Li-ion) batteries for 2024–2040 are similar to those published by Schmidt and his group from Imperial College London [47]. They estimated low, average, and high-cost values for various energy storage technologies, including Li-ion batteries, whose experience rate is projected to be $12 \pm 3\%$ during 2024–2040.

Any referenced costs in this study quoted in dollars of other years are adjusted to 2018-dollar values using Consumer Price Index (CPI-U) data provided by the U.S. Department of Labor/Bureau of Labor Statistics [48].

To ensure there is enough power generation capacity to satisfy electricity demand reliably (i.e., to ensure resource adequacy), it is assumed that installed power generation capacity must exceed the expected peak load by 12% [19]. Similarly, to ensure operational reliability, it is assumed that each isolated network must permanently have power generation spinning reserves equal to the maximum between the capacity of the largest synchronized unit and the sum of 3% of the total demand and 5% of total renewable energy, as recommended by the 3 + 5 rule of NREL [49].

2.3. Grid Interconnection Evaluation

The PSSE simulation model, developed by Siemens PTI, was used to represent the interconnected KSA grid in 2020, with the assumption that all the current plans to expand the transmission system have been implemented. The modeled system consists of 362 high-voltage buses (mostly 380 KV buses), 793 power generators, and 1732 transmission lines with a total length of 112,430 km. To this baseline system of 2020, we added an interconnection to the isolated areas. A simulation of this modified power system provided information on the generation and transmission capacity requirements to maintain reliability during peak load times. The main-grid-extension (MGE) costs were calculated for each isolated area. These costs represent capital costs, generation costs, fixed and variable operation, maintenance costs, and emissions damage costs under all the scenarios described in Section 2.4.

2.4. Optimal Off-Grid Distributed Generation Mix

An off-grid distributed generation (DG) system has been evaluated as an alternative to the grid extension, considering all feasible electricity generation technologies. A mixed-integer linear program (MILP) model has been developed to determine, yearly, the optimal selection and size of new equipment to meet hourly demand and ancillary services requirements at each isolated network. Consistent with the energy resources available in KSA, the model assumes that the only sources of distributed power generation that can be installed are solar PV, wind, diesel, oil, and HFO engines, and lithium-ion batteries for energy storage.

The objective of the MILP is to minimize the total costs of installing new power plants, running the generators (generation fuel costs, spinning reserve fuel costs, start-up costs, fixed no-load costs, and social costs of air emissions) and any penalties (over-generation, under-generation, un-met spinning reserves) for the three areas considered, during the planning horizon. The decision variables and parameters are listed in the box below, and the objective function to minimize is:

$$\begin{aligned} \min z = & \sum_{n=1}^N \left(\sum_{y=1}^T \left(\text{Build}_{u,y,n} \times \left(C_{u,y,n}^{\text{cap}} \times \text{FCF} + C_{u,y,n}^{\text{O\&M}} \right) + \sum_{i=1}^2 i_{y,n}^{\text{size}} \times \left(C_{i,y,n}^{\text{cap}} \times \text{FCF} + C_{i,y,n}^{\text{O\&M}} \right) + \text{ES}_{y,n}^{\text{size}} \times \right. \right. \\ & \left. \left(C_{y,n}^{\text{EScap}} \times \text{FCF} + C_{y,n}^{\text{ESO\&M}} \right) + \left(\sum_{t=1+(y-1)*H}^{H \times y} \sum_{u=1}^U \left(G_{u,t,n} \times C_{u,t,n}^{\text{fuel}} + \text{SR}_{u,t,n} \times C_{u,t,n}^{\text{SR}} + C_{u,t,n}^{\text{Start}} + G_{u,t,n} \times \right. \right. \right. \\ & \left. \left. \left(\text{CO}_{2,u,n} \times C_t^{\text{CO}_2} + \text{N}_2\text{O}_{u,n} \times C_t^{\text{N}_2\text{O}} + \text{CH}_{4,u,n} \times C_t^{\text{CH}_4} \right) + G_{t,n}^{\text{surplus}} \times C_g^{\text{penalty}} + G_{t,n}^{\text{short}} \times C_g^{\text{penalty}} + \text{SR}_{t,n}^{\text{short}} \times \right. \right. \\ & \left. \left. C_{\text{SR}}^{\text{penalty}} + \text{NSR}_{t,n}^{\text{short}} \times C_{\text{NSR}}^{\text{penalty}} \right) \right) \end{aligned}$$

MILP to optimally design the off-grid system

Sets and indexes

Ψ^U	Set of fossil-fuel-fired power generation units. Indexed by $u \in \{1, 2, \dots, U\}$
Ψ^I	Set of variable renewable energy types (i.e., intermittent) power generators. Indexed by $i \in \{1 = \text{PV}, 2 = \text{wind}\}$
Ψ^N	Set of isolated power networks/areas. Indexed by $n \in \{1, 2, 3\}$
Ψ^T	Set of hours in the planning horizon. Indexed by $t \in \{1, 2, \dots, 8760 \times 20\}$
Ψ^Y	Set of years in the planning horizon. Indexed by $y \in \{1, 2, \dots, 20\}$

Constants

T	Number of intervals in the time horizon; equals 20
H	Number of hours in one year; equals 8760
M	Large positive constant number (e.g., 10^6)

Decision Variables

$\text{Build}_{u,y,n}$	Equals 1 if power generation unit u is built in year y at area n and equals 0 otherwise
$u_{t,n}^{\text{status}}$	Equals 1 if unit u is committed to operating in time t at area n
$G_{u,t,n}$	Power generation [MW] from unit u in time t at area n
$G_{i,t,n}$	Power generation [MW] from units type i in time t at area n
$\text{SR}_{u,t,n}$	Spinning reserve [MW] provided by unit u in interval t at area n
$\text{SR}_{t,n}^{\text{ES}}$	Spinning reserve [MW] provided by battery energy storage in interval t at area n
$\text{NSR}_{u,t,n}$	Non-spinning reserve [MW] provided by unit u in interval t at area n
$G_{t,n}^{\text{surplus}}$	Surplus of generation over demand [MW] in interval t at area n
$G_{t,n}^{\text{short}}$	Shortage of generation below demand [MW] in interval t at area n
$\text{SR}_{t,n}^{\text{short}}$	Shortage of spinning reserve below requirement [MW] in interval t at area n
$\text{NSR}_{t,n}^{\text{short}}$	Shortage of non-spinning reserve below requirement [MW] in interval t at area n
$i_{y,n}^{\text{size}}$	Size in MW of renewable energy ($i = 1$ for solar PV and $i = 2$ for wind turbine) in year y at area n
$\text{ES}_{y,n}^{\text{size}}$	Size of energy storage (MW) in year y at area n
$\text{ES}_{t,n}$	Quantity of energy storage (MWh) in time t at area n
$\text{ES}_{t,n}^{\text{disch}}$	Quantity of energy discharged from energy storage (MWh) in time t at area n
$\text{ES}_{t,n}^{\text{disch_st}}$	Energy storage discharge status. Equals 1 if the battery is discharging energy during time t at area n and equals 0 if it is not discharging
$\text{ES}_{t,n}^{\text{ch}}$	Quantity of energy charged to energy storage (MWh) in time t at area n
$\text{ES}_{t,n}^{\text{ch_st}}$	Energy storage charge status. Equals 1 if the battery is charging energy during time t at area n and equals 0 if it is not charging
$\text{SR}_{t,n}^{\text{min}}$	Quantity of spinning reserves [MW] required in interval t at area n
Parameters	
$C_{u,t,n}^{\text{start}}$	Cost of starting up unit u [\$] in interval t at area n
D_t	System power demand in interval t [MW]
$D_{t,n}$	System power demand [MW] in interval t at area n
$\text{NSR}_{t,n}^{\text{min}}$	Quantity of non-spinning reserves [MW] required in interval t at area n
C_g^{penalty}	Penalty cost of the system's over/under generation [\$/MWh]
$C_{\text{SR}}^{\text{penalty}}$	Penalty cost of system's spinning reserve shortage [\$/MWh]
$C_{\text{NSR}}^{\text{penalty}}$	Penalty cost of system's non-spinning reserve shortage [\$/MWh]
$C_{u,t,n}^{\text{fuel}}$	Marginal cost [\$/MWh] of operating unit u in interval t at area n

Parameters	
$C_{u,t,n}^{SR}$	Cost of spinning reserves [\$/MWh] provided by unit u in interval t at area n
$C_{u,t,n}^{cap}$	Capital costs or CapEx (\$) incurred to build generation unit u in time t at isolated area n .
FCF	Fixed Charge Factor, a.k.a Fixed Charge Rate. Multiplying CapEx by FCF yields the annualized capital costs
$C_{u,t,n}^{O\&M}$	fixed operation and maintenance cost [\$/MW] of operating unit u in interval t at area n
$C_{u,t,n}^{st}$	Start-up cost [\$] of unit u in interval t at area n
$C_{t,n}^{ES_cap}$	Capital costs or CapEx (\$/MW) incurred to install energy storage in time t at isolated area n .
$C_{t,n}^{ES_O\&M}$	Fixed operation and maintenance cost [\$/MW] of operating energy storage in interval t at area n
$C_t^{CO_2}$	Social cost of carbon dioxide emissions (\$/tonne) in time t
$C_t^{N_2O}$	Social cost of nitrous oxide emissions (\$/tonne) in time t
$C_t^{CH_4}$	Social cost of methane emissions (\$/tonne) in time t
$G_{u,n}^{max}$	Maximum generation [MW] of unit u at area n
$G_{u,n}^{min}$	Minimum generation [MW] of unit u at area n
$G_{i,t,n}^{max}$	Forecasted generation [MW] of intermittent source i in interval t at area n
$R_{u,n}^{ur}$	Maximum ramp-up rate of generator u [MW/Hour] at area n
$R_{u,n}^{dr}$	Maximum ramp-down rate of generator u [MW/Hour] at area n
$UT_{u,n}^{min}$	Minimum uptime of unit u [number of intervals] at area n
$DT_{u,n}^{min}$	Minimum downtime of unit u [number of intervals] at area n
$UT_{0,u,n}^{min}$	Initial minimum uptime of unit u [number of intervals] at area n
$DT_{0,u,n}^{min}$	Initial minimum downtime of unit u [number of intervals] at area n
$CF_{u,n}$	Annual capacity factor of unit u at area n
η_i^{deg}	Annual efficiency degradation rate (%)
η_{ES}^{ch}	Energy storage charging efficiency (%)
η_{ES}^{disch}	Energy storage discharging efficiency (%)
ES_{rate}^{ch}	Maximum energy storage charging/discharging rate (%)
ES_{cap}^{min}	Minimum energy storage capacity (%)
CO_{2u}	Carbon dioxide emissions rate (tonne/MWh) from unit u
N_2O_u	Nitrous oxide emissions rate (tonne/MWh) from unit u
CH_{4u}	Methane emissions rate (tonne/MWh) from unit u

The optimization objective function is subject to the following operational and technical constraints:

1. The total annual electricity generation from fossil-fuel-fired units and variable renewable energy, plus the energy discharged from the battery, must equal demand plus energy charging the battery. Any shortage or surplus is quantified and penalized in the objective function:

$$\sum_{u=1}^U G_{u,t,n} + \sum_{i=1}^2 G_{i,t,n} + ES_{t,n}^{disch} - ES_{t,n}^{ch} - G_{t,n}^{surplus} + G_{t,n}^{short} \geq D_{t,n} \quad \forall t, n$$

2. The spinning reserves provided by generators or batteries must be above the minimum requirement. If not, the shortage in spinning reserves is calculated and penalized in the objective function:

$$\sum_{u=1}^U SR_{u,t,n} + SR_{t,n}^{short} + SR_{t,n}^{ES} \geq SR_{t,n}^{min} \quad \forall t, n$$

3. The spinning reserve requirements are equal to or exceed the maximum between 3% of electricity demand plus 5% of the renewable energy systems' electricity and the capacity of the largest synchronized (i.e., scheduled to produce) generator:

$$SR_{t,n}^{min} \geq \max(0.03 \times D_{t,n} + \sum_{i=1}^2 0.05 \times G_{i,t,n}, G_{u,n}^{max} \times u_{t,n}^{status}) \quad \forall u, t, n$$

4. The non-spinning reserves provided by generators must equal or exceed a minimum requirement (which is equal to 12% of the area's electricity demand) [19]:

$$\sum_{u=1}^U \text{NSR}_{u,t,n} + \text{NSR}_{t,n}^{\text{short}} \geq \text{NSR}_{t,n}^{\text{min}} \quad \forall t, n$$

5. The power generation from conventional generators must be between their minimum and maximum limits:

$$G_{u,t,n} + \text{SR}_{u,t,n} \leq G_{u,n}^{\text{max}} \times u_{t,n}^{\text{status}} \quad \forall u, t, n$$

$$G_{u,t,n} \geq G_{u,n}^{\text{min}} \times u_{t,n}^{\text{status}} \quad \forall u, t, n$$

6. The total electricity supplied from each fossil-fuel-fired unit each year is limited by the product of its generation capacity and capacity factor:

$$\sum_{h=1+(y-1) \times H}^{H \times y} (G_{u,h,n} + \text{SR}_{u,h,n}) \leq G_{u,n}^{\text{max}} \times H \times \text{CF}_{u,n} \quad \forall u, h, y, n$$

7. Start-up costs are incurred when a power-generating unit passes from being offline to being online:

$$C_{u,t,n}^{\text{start}} \geq C_{u,t,n}^{\text{st}} \times (u_{t,n}^{\text{status}} - u_{t-1,n}^{\text{status}}) \quad \forall u, t, n$$

8. The power generators must operate within the limits of their capability to ramp up and ramp down their production:

$$G_{u,t,n} - G_{u,t-1,n} \leq R_{u,n}^{\text{ur}} \quad \forall u, t, n$$

$$-G_{u,t,n} + G_{u,t-1,n} + \text{SR}_{u,t-1,n} \leq R_{u,n}^{\text{dr}} \quad \forall u, t, n$$

$$\text{SR}_{u,t,n} \leq R_{u,n}^{\text{ur}} \quad \forall u, t, n$$

9. The power generation from variable renewable energy sources is bounded by their installed capacity:

$$G_{i,h+(y-1) \times H,n} \leq i_{y,n}^{\text{size}} \quad \forall i, n, h, y$$

10. The power generation from solar PV and wind farms cannot be more than their installed power generation capacity adjusted by annual degradation:

$$G_{i,h+y \times H,n} \leq (i_{y,n}^{\text{size}} - i_{y-1,n}^{\text{size}}) + \eta_i^{\text{deg}} \times G_{i,h+(y-1) \times H,n} \quad \forall i, h, y, n$$

11. The fossil-fuel-fired power generators operate within their minimum up-time and minimum downtime limits:

$$\sum_{t=1}^{UT_{0,u,n}^{\text{min}}} (1 - u_{t,n}^{\text{status}}) = 0 \quad \forall u, t, n$$

$$\sum_{m=t}^{t+UT_{u,n}^{\text{min}}-1} u_{m,n}^{\text{status}} \geq UT_{u,n}^{\text{min}} \times (u_{t,n}^{\text{status}} - u_{t-1,n}^{\text{status}}) \quad \forall u, n, t \in [UT_{0,u,n}^{\text{min}} + 1, T \times H - UT_{u,n}^{\text{min}} + 1]$$

$$\sum_{m=t}^{T \times H} (u_{m,n}^{\text{status}} - (u_{t,n}^{\text{status}} - u_{t-1,n}^{\text{status}})) \geq 0 \quad \forall u, n, t \in [T \times H - UT_{u,n}^{\text{min}} + 2, T \times H]$$

$$\sum_{t=1}^{DT_{0,u,n}^{\text{min}}} u_{t,n}^{\text{status}} = 0 \quad \forall u$$

$$\sum_{m=t}^{t+DT_{u,n}^{\text{min}}-1} (1 - u_{m,n}^{\text{status}}) \geq DT_{u,n}^{\text{min}} \times (u_{t-1,n}^{\text{status}} - u_{t,n}^{\text{status}}) \quad \forall u, n, t \in [DT_{0,u,n}^{\text{min}} + 1, T \times H - DT_{u,n}^{\text{min}} + 1]$$

$$\sum_{m=t}^{T \times H} ((1 - u_{m,n}^{\text{status}}) - (u_{t-1,n}^{\text{status}} - u_{t,n}^{\text{status}})) \geq 0 \quad \forall u, n, t \in [T \times H - DT_{u,n}^{\text{min}} + 2, T \times H]$$

12. The energy stored in the battery is equal to the energy stored in the prior period plus the energy charged from the grid minus the energy discharged to the grid:

$$ES_{t,n} - ES_{t-1,n} \leq ES_{t,n}^{ch} \times \eta_{ES}^{ch} - (ES_{t,n}^{disch} + SR_{t,n}^{ES}) \div \eta_{ES}^{disch} \quad \forall t, n$$

13. The charge and discharge rates of the battery do not exceed its maximum physical limit. The energy discharged is also constrained by the provision of spinning reserves:

$$ES_{h+(y-1) \times H, n}^{disch} + SR_{h+(y-1) \times H, n}^{ES} \leq ES_{rate}^{ch} \times ES_{y,n}^{size} \quad \forall h, y, n$$

$$ES_{h+(y-1) \times H, n}^{ch} \leq ES_{rate}^{ch} \times ES_{y,n}^{size} \quad \forall h, y, n$$

14. The level of energy stored in the batteries must be between the maximum and minimum design limits at all times:

$$ES_{h+(y-1) \times H, n} \leq ES_{y,n}^{size} \quad \forall h, y, n$$

$$ES_{h+(y-1) \times H, n} \geq ES_{cap}^{min} \times ES_{y,n}^{size} \quad \forall h, y, n$$

15. The binary variable indicating if a battery is charging should equal 1 when energy goes into the battery. The binary variable indicating that the battery is in discharging mode should equal 1 when the battery is discharging energy into the grid or providing spinning reserves, or both:

$$M \times (1 - ES_{t,n}^{ch_st}) \geq ES_{t,n}^{disch} + SR_{t,n}^{ES} \quad \forall t, n$$

$$M \times ES_{t,n}^{ch_st} \geq ES_{t,n}^{ch} \quad \forall t, n$$

$$M \times (1 - ES_{t,n}^{disch_st}) \geq ES_{t,n}^{ch} \quad \forall t, n$$

$$M \times ES_{t,n}^{disch_st} \geq ES_{t,n}^{disch} + SR_{t,n}^{ES} \quad \forall t, n$$

16. At all times, the battery should be in either charging or discharging mode:

$$ES_{t,n}^{ch_st} + ES_{t,n}^{disch_st} \leq 1 \quad \forall t, n$$

17. All decision variables are non-negative:

$$G_{u,t,n}, SR_{u,t,n}, C_{u,t,n}^{start}, SR_{t,n}^{short}, NSR_{t,n}^{short}, I_{y,n}^{size}, ES_{y,n}^{size},$$

$$ES_{t,n}^{disch}, ES_{t,n}^{ch}, SR_{t,n}^{ES}, G_{t,n}^{surplus}, C_{t,n}^{short} \geq 0$$

The optimization model is solved using CPLEX in the AMPL environment. A solution to this model will specify, for each year, the optimal installed capacity of each type of technology considering three (3) scenarios that vary fuel prices, solar and wind costs, energy storage costs, and emissions costs. The total costs calculated by this model will determine whether grid extension or off-grid DG is the least-cost option to supply the total electricity demand at each isolated area across the 2024–2040 planning horizon.

2.5. Scenarios to Explore Results' Sensitivity to Assumptions

The simulations are conducted for three scenarios that vary in assumptions regarding future fuel prices, costs of air emissions, and capital costs of solar, wind, and energy storage technologies, as described in Table 4.

Table 4. Scenarios to explore the sensitivity of results to assumptions on fuel prices, cost and performance of electricity generation technologies, and cost of carbon dioxide emissions.

Parameter	Scenario	Reference	Renewables Favorable	Fossil-Fuels Favorable
Oil prices [\$/Bbl]		ref case 2016 OPEC	High price case 2016 OPEC	Low price case 2016 OPEC
Cost of Carbon Emissions [\$/tonne]		SCC assuming a 3% discount rate [45]	SCC assuming a 2.5% discount rate [45]	SCC assuming a 5% discount rate [45]
Solar PV capital costs [\$/kW]		NREL ATB middle scenario	NREL ATB low scenario	NREL ATB high scenario
Wind turbine capital cost (\$/kW)		NREL ATB mid scenario	NREL ATB low scenario	NREL ATB high scenario
Li-ion battery capital cost (\$/kW)		Average scenario in [47]	Low scenario in [47]	High scenario in [47]

3. Results and Discussion

Figure 1 presents the total costs to provide electricity to each remote area over the 2024–2040 planning horizon by either extending the primary grid (MGE option) or the off-grid distribution generation (DG) option under all scenarios. The yellow dashes indicate MGE costs when oil-fired CCPPs power the grid, which is the most likely case. The gray dashes indicate MGE costs assuming gas-fired CCPPs power the primary grid. The DG option’s total costs are shown in blue-colored bars. These costs correspond to the optimal integrated resource plan to provide electricity to the remote loads using distributed generation as determined by the MILP model summarized in Section 2.3. Complete MILP results are presented in Supplementary S3.

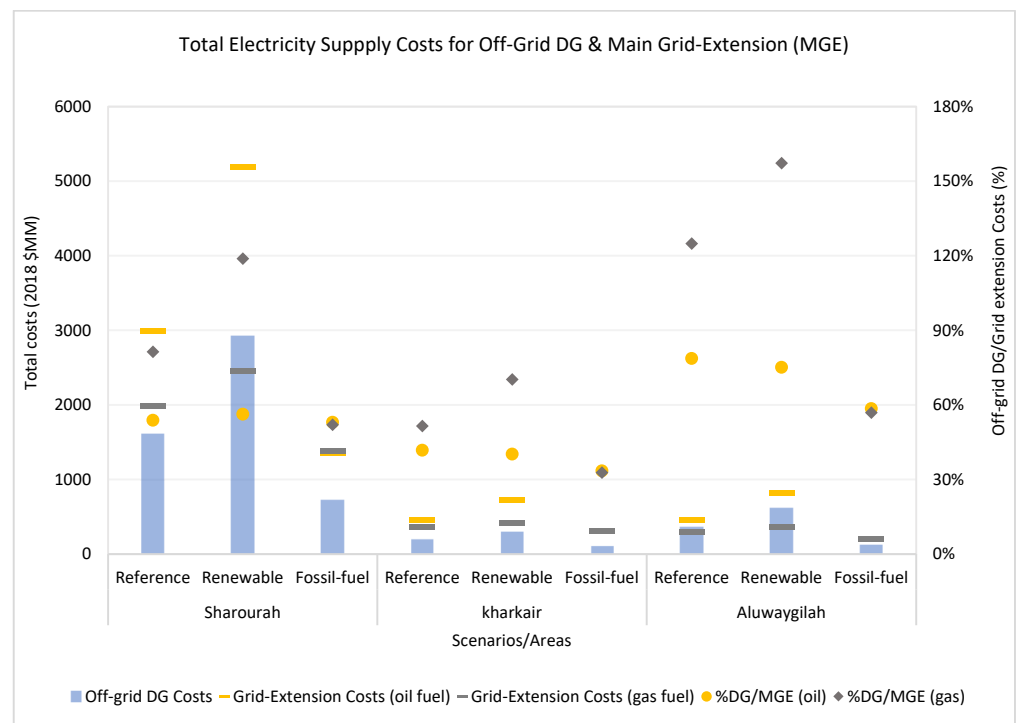


Figure 1. Total costs of supplying electricity to the remote areas by either off-grid DG or the main-grid extension (fueled by oil or gas) under all scenarios. The yellow circles and gray diamonds indicate the cost ratio of off-grid DG to the primary grid extension fueled by oil and gas, respectively.

In Figure 1, the yellow circles represent the cost ratio (%) of off-grid DG to MGE-oil (i.e., assuming the primary grid is powered by an oil-fired CCPP). The gray diamonds represent

the cost ratio (%) of off-grid DG to MGE-gas, assuming the primary grid is powered by a gas-fired CCPP. The results show that the off-grid DG option is more economical under all scenarios and for all areas than the MGE-oil option. It is also clear that the longer the necessary transmission lines to connect to the primary grid, the more economical the off-grid DG option is. For the Kharkhir area, the most remote location, the advantage of off-grid DG is significant; its costs are only 35–40% of the MGE-oil's costs. For Sharorah, the second most remote area, off-grid DG costs are 45–50% lower. For the Uwayqilah area, which requires transmission lines less than half as long as the other areas, off-grid DG costs are 20–40% lower than MGE.

It is also noticeable that the ratio between the costs of off-grid DG and MGE-oil, represented by the yellow dots, is almost the same under the reference and renewable scenarios for all areas. This is because the increase in the MGE-oil costs is similar to the rise in the off-grid DG costs. Under the renewable scenario, the MGE costs are high due to increased fuel prices and costly emissions charges. Similarly, the off-grid DG costs are also increased due to the larger share of solar and wind energy, which grows from 10–20% under the Reference scenario to about 35–50% of the energy mix under the Renewable scenario (see Supplementary S3.3). However, contrary to what could be expected, under a fossil-fuel scenario, low fossil fuel prices favor the economics of the off-grid DG. This is because as fuel prices decline, the costs of extending the transmission lines become a more significant component of the total cost of implementing the MGE option. At the same time, the off-grid DG benefits increase with low fuel prices.

The analysis has shown that the off-grid option is a better alternative and that assumptions made about oil prices have minimal impact on this result. Indeed, if average oil prices in 2024–2040 dropped from 81 USD/bbl under the reference scenario to 24 USD/bbl under the fossil-fuel scenario, the economics of the off-grid option would improve.

To find the conditions that would make grid extension more economical in these remote areas, we consider a case in which natural gas is used instead of oil as the primary fuel for the grid-connected combined cycle power plant (CCPP). Interestingly, under this assumption, the high fuel prices and low PV and wind capital costs assumed under the renewable scenario would lower the MGE-gas costs relative to the off-grid option's costs for Sharorah and Uwayqilah. The gray diamonds indicate this in Figure 1, which are above the 100% mark for the two areas under the renewable scenario. Under the renewable scenario, the ratio of oil prices to natural gas prices is, on average, 27, while it is 17 and 6 under the reference and fossil fuel scenarios, respectively. The position of the gray dots shows that high oil-to-natural gas price ratios vastly improve the economics of grid extension relative to the off-grid DG option. This is because the DG's optimal energy mix includes at least 50% of HFO, a fuel highly priced under this scenario (see Supplementary S3.3). Likewise, under the reference scenario, MGE-gas is more cost-effective for Uwayqilah due to its short distance from the primary grid. However, for Sharorah, MGE-gas's cost is 15% higher than off-grid DG's, influenced more by the long distance from the primary grid. On the other hand, under the fossil-fuel scenario (i.e., low fuel prices), the off-grid DG is the least-cost option for all areas because of the low cost of oil relative to gas. It is also worth noting that the low oil-to-gas price ratio results in almost the same total costs for the main-grid-extension (MGE) option powered by either gas-fired CCPP or oil-fired CCPP.

In Kharkhir, unlike other areas, the off-grid option is significantly more economical under all scenarios due to its low load and extreme distance from the primary grid. The MGE-gas performance is somewhat better under the renewable scenario where the cost of off-grid DG is still lower than the MGE-gas, but only by 30%.

The off-grid DG option assessment also presents interesting findings regarding the levelized cost of electricity and the optimal energy mix. The results reveal that lower HFO fuel prices reduce the HFO engine's marginal costs significantly, making these the most cost-effective fossil-fired power generation technology (see Supplementary S3.2). This finding is impressive given the high capital and fixed costs of HFO engines relative to diesel engines. However, the optimal energy mix contains a small share of power generation from

diesel engines which are an economical alternative to satisfy spinning and non-spinning reserve requirements (see Supplementary S3.3). Results also show that the new GE wind technology, with its high efficiency and expected capital cost reductions, makes the cost of wind-powered electricity very competitive with fossil fuels. This happens despite the unimpressive wind resources of Sharorah, Kharkhir, and Uwayqilah, where the capacity factors of GE wind turbines installed at 92 m are just 24%, 26%, and 29%, respectively.

Although wind energy supplies a larger share of energy, solar PV is the least-cost option under the reference and renewable scenarios. At the same time, the HFO engine is the least-cost option under the fossil-fuel scenario.

The results indicate that due to their low levelized cost of electricity, both solar and wind will provide a considerable share of the electricity in all areas under the reference and the renewable scenarios. Under the reference scenario, their percentage ranges from 20% in Sharorah to 35% in Kharkhir. These figures are increased under the renewable scenario to 40% and 50%, respectively. Under the reference and renewable scenarios, the average annual wind and PV curtailment ranges from 5% in Sharorah to 9% in Kharkhir. The hourly generation profiles demonstrate that solar PV and wind units perform best during spring but produce much less electricity output during summer when loads in these isolated areas peak.

One more finding worth mentioning is that, under all scenarios and in all areas, energy storage technology costs are 40% higher than those from renewable or fossil-fuel generators. This is because of the high capital costs of storage relative to the costs of solar PV, wind, and efficient HFO/diesel engines (see Supplementary S3.2).

Finally, the results demonstrate the importance of analyzing grid operations at granular temporal resolution. In this paper, we considered hourly data to represent the fluctuations in load and renewable energy and to properly account for the technical operating constraints of the conventional generators (such as ramp-rate limits, start-up times, and minimum downtime and uptime requirements). The results obtained are significantly different from those derived from an analysis that uses daily resolution. Figure 2 shows that using daily data—i.e., ignoring the inter-hour fluctuations in the energy output from the off-grid wind and solar resources—would mistakenly suggest a lower requirement for the installed capacity of those resources. This would put the system at risk of insufficient ability to meet demand. This erroneous analysis would suggest that the off-grid development is much more economical than initially calculated. For instance, the cost ratios of off-grid DG to MGE-gas in Sharorah and Uwayqilah calculated under the reference scenarios are reduced from 81% and 125% to 55% and 94%, respectively, if daily generation and load data are used instead of hourly generation. Thus, an hourly representation of the system is critical for adequately determining the optimal energy mix and cost assessment.

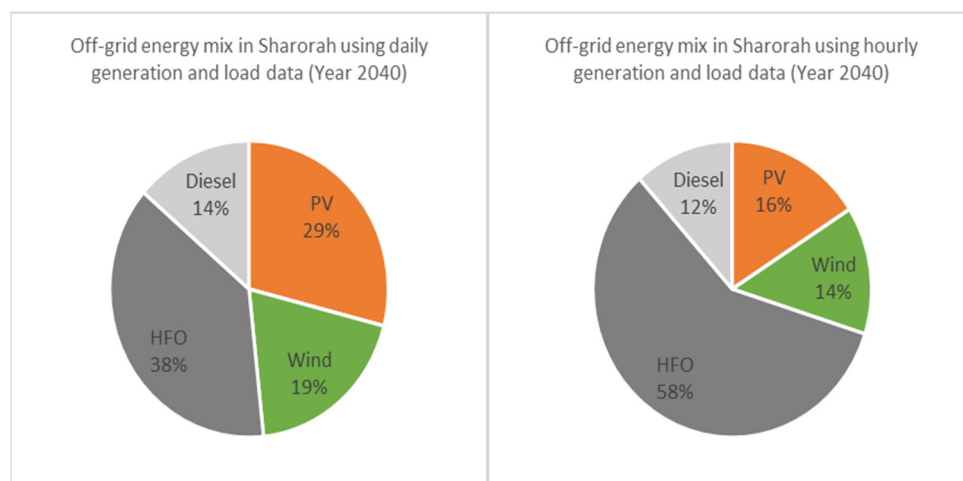


Figure 2. Comparison of off-grid energy mix in Sharorah using daily versus hourly simulated generation and load data.

4. Conclusions

This study illustrates an analysis to compare two very distinct alternatives for providing electricity to remote areas: grid extension vs. distributed generation. While the same level of reliability can be achieved with both options through the installation of the proper power generation capacity, the costs can differ significantly depending on the distance from the grid, availability of renewables, and the energy resource mix of the electricity transmitted through the central grid.

Exploring the options to meet electricity demand in three remote, isolated microgrid systems in Saudi Arabia reveals a great opportunity to economically integrate large shares of renewable energy from solar and wind under most scenarios considered. Developing an off-grid solar DG system including PV, wind, and/or efficient HFO/diesel engines is the best alternative to serve the three remote areas under most scenarios that account for uncertainties in fuel, technologies, and social costs of greenhouse-gas emissions. Under a scenario that makes the deployment of renewables highly attractive, the least-cost energy mix includes more than 250 MW of off-grid solar PV and wind systems. Thus, the regions isolated from the primary power grid of Saudi Arabia are excellent venues for deploying a good portion of the renewable electricity generation capacity the country plans to install over the next decade as part of Vision 2030 [16,18].

Supplementary Materials: The following supporting information can be downloaded at: <https://www.mdpi.com/article/10.3390/en16020958/s1>, Table S1: Characteristics of the existing power plants; Table S2: Greenhouse emissions rates from fuel combustion; Table S3: Average of hourly data on solar resources and climate conditions in isolated areas observed in 2016; Table S4: Wind data summary for the isolated areas; Table S5: Summary of previous studies' scope, methodology, and findings; Figure S1: LCOE of grid-connected power generation technologies under all scenarios assuming excellent solar and wind resources in KSA (GHI of 2308 kWh/m²/year, wind speed of 7.46 m/s), 52% fuel efficient CCPP with 87% capacity factor, nominal WACC of 7%, 2% inflation and 1.5% insurance charges; Figure S2: LCOE of off-grid power generation technologies at Sharorah under all scenarios; Figure S3: LCOE of off-grid power generation technologies at Kharkhir under all scenarios; Figure S4: LCOE of off-grid power generation technologies at Uwayqilah under all scenarios; Figure S5: Annual electricity generation by fuel and annual cumulative capacity addition in Sharorah under all scenarios; Figure S6: Annual electricity generation by fuel and annual cumulative capacity addition in Kharkhir under all scenarios; Figure S7: Annual electricity generation by fuel and annual cumulative capacity addition in Uwayqilah under all scenarios. (References [6–12,25,30,32,50–58] are cited in the supplementary materials).

Author Contributions: Conceptualization, B.J.A. and D.P.-E.; methodology, B.J.A.; software, B.J.A.; investigation, B.J.A.; resources, B.J.A.; data curation, B.J.A.; writing—original draft preparation, B.J.A.; writing—review and editing, D.P.-E.; visualization, B.J.A.; supervision, D.P.-E.; funding acquisition, D.P.-E. and B.J.A. All authors have read and agreed to the published version of the manuscript.

Funding: This research received funding from the Center for Climate and Energy Decision Center, funded by the U.S. National Science Foundation (SES-0949710).

Data Availability Statement: Data available upon request.

Conflicts of Interest: The authors declare no conflict of interest.

References

1. United Nations. Report: Universal Access to Sustainable Energy Will Remain Elusive Without Addressing Inequalities. 2021. Available online: <https://www.un.org/sustainabledevelopment/blog/2021/06/report-universal-access-to-sustainable-energy-will-remain-elusive-without-addressing-inequalities/> (accessed on 16 November 2022).
2. Thushara, D.S.M.; Hornberger, G.M.; Baroud, H. Decision analysis to support the choice of a future power generation pathway for Sri Lanka. *Appl. Energy* **2019**, *240*, 680–697. [CrossRef]
3. Trottera, P.A.; Cooper, N.J.; Wilson, P.R. A multi-criteria, long-term energy planning optimisation model with integrated on-grid and off-grid electrification—The case of Uganda. *Appl. Energy* **2019**, *243*, 288–312. [CrossRef]
4. Moretti, L.; Astolfi, M.; Vergara, C.; Macchi, E.; Pérez-Arriaga, J.I.; Manzolini, G. A design and dispatch optimization algorithm based on mixed integer linear programming for rural electrification. *Appl. Energy* **2019**, *233–234*, 1104–1121. [CrossRef]

5. Nock, D.; Levin, T.; Baker, E. Changing the policy paradigm: A benefit maximization approach to electricity planning in developing countries. *Appl. Energy* **2020**, *264*, 114583. [CrossRef]
6. Molyneaux, L.; Wagner, L.; Foster, J. Rural electrification in India: Galilee Basin coal versus decentralized renewable energy micro grids. *Renew. Energy* **2016**, *89*, 422–436. [CrossRef]
7. Thiam, D.-R. Renewable decentralized in developing countries: Appraisal from microgrids project in Senegal. *Renew. Energy* **2010**, *35*, 1615–1623. [CrossRef]
8. Luta, D.N.; Raji, A.K. Decision-making between a grid extension and a rural renewable off-grid system with hydrogen generation. *Int. J. Hydrogen Energy* **2018**, *43*, 9535–9548. [CrossRef]
9. Golbarg Rohani, M.N. Techno-economical analysis of stand-alone hybrid renewable power system for Ras Musherib in United Arab Emirates. *Energy* **2014**, *64*, 828–841. [CrossRef]
10. Zeyringer, M.; Pachauri, S.; Schmid, E.; Schmidt, J.; Worrell, E.; Morawetz, U.B. Analyzing grid extension and stand-alone photovoltaic systems for the cost-effective electrification of Kenya. *Energy Sustain. Dev.* **2015**, *25*, 75–86. [CrossRef]
11. Szabó, S.; Bódis, K.; Huld, T.; Moner-Girona, M. Sustainable energy planning: Leapfrogging the energy poverty gap in Africa. *Renew. Sustain. Energy Rev.* **2013**, *28*, 500–509. [CrossRef]
12. Deichmann, U.; Meisner, C.; Murray, S.; Wheeler, D. The economics of renewable energy expansion in rural Sub-Saharan Africa. *Energy Policy* **2011**, *39*, 215–227. [CrossRef]
13. SEC At Glance. SEC Official Webpage. Available online: <https://www.se.com.sa/en-us/invshareholder/Pages/BackgroundOnBusinessSegment.aspx> (accessed on 2 November 2022).
14. Saudi Electricity Company. 2019 Annual Report. 2020. Available online: <https://www.se.com.sa/en-us/Pages/AnnualReports.aspx> (accessed on 5 November 2022).
15. Water & Electricity Regulatory Authority (WERA). Annual Statistical Booklet for Electricity and Seawater Desalination Industries. 2019. Available online: <https://wera.gov.sa/Statistics/> (accessed on 20 November 2022).
16. Government of Saudi Arabia. Saudi Arabia's Vision 2030. 2016. Available online: <http://vision2030.gov.sa/en/media-center> (accessed on 20 October 2022).
17. ACWA Power. Rabigh 2 IPP: Project News. Available online: <https://www.acwapower.com/en/projects/rabigh-2-ipp/> (accessed on 25 October 2022).
18. The National Renewable Energy Program. 2018. Available online: <https://www.powersaudi Arabia.com.sa/web/index.htm> (accessed on 5 November 2022).
19. Government of Saudi Arabia. National Transformation Program. 2016. Available online: http://vision2030.gov.sa/sites/default/files/NTP_En.pdf (accessed on 25 October 2022).
20. Pletka, R.; Khangura, J.; Rawlins, A.; Waldren, E.; Wilson, D. *Capital Costs for Transmission and Substations*; 2019 Update, Report prepared by Black & Veatch Corporation for Western Electric Coordinating Council (WECC); Black & Veatch Corporation: Overland Park, KS, USA, 2019; p. 56.
21. US Energy Information Administration. Cost and Performance Characteristics of New Generating Technologies. In *Annual Energy Outlook 2019*; US Energy Information Administration (EIA): Washington, DC, USA, 2019; p. 3.
22. Wärtsilä. *Energy Exemplar, Power System Optimization by Increased Flexibility*; Wärtsilä Corporation: Helsinki, Finland, 2014.
23. Rajagopalan, M.; Gandotra, S. Fuel-flexible, efficient generation using internal combustion engines (ICEs) to meet growing demand in Myanmar. In *Powergen ASIA 2015*; Wärtsilä India Pvt. Ltd.: Mumbai, India, 2015.
24. Energy and Environmental Economics, Inc. *Capital Cost Review of Generation Technologies*; Energy and Environmental Economics, Inc.: San Francisco, CA, USA, 2014; Available online: https://www.wecc.biz/Reliability/2014_TEPPC_Generation_CapCost_Report_E3.pdf (accessed on 10 November 2022).
25. EPA. Emission Factors for Greenhouse Gas Inventories. 2015. Available online: https://www.epa.gov/sites/production/files/2015-11/documents/emission-factors_nov_2015.pdf (accessed on 2 November 2022).
26. Feldman, D.; Vignesh, R.; Fu, R.; Ramdas, A.; Desai, J.; Margolis, R. *U.S. Solar Photovoltaic System Cost Benchmark: Q1 2020*; NREL/TP-6A20-77324; National Renewable Energy Laboratory: Golden, CO, USA, 2021. Available online: <https://www.nrel.gov/docs/fy21osti/77324.pdf> (accessed on 2 November 2022).
27. Jordan, D.C.; Kurtz, S.R. Photovoltaic Degradation Rates-an Analytical Review. *Prog. Photovolt.* **2013**, *21*, 12–29. [CrossRef]
28. Holbert, K.E. Solar Calculations. 2007. Available online: <http://holbert.faculty.asu.edu/eee463/SolarCalcs.pdf> (accessed on 2 November 2022).
29. Alqahtani, B.J.; Holt, K.M.; Patiño-Echeverri, D.; Pratson, L. Residential Solar PV Systems in the Carolinas: Opportunities and Outcomes. *Environ. Sci. Technol.* **2016**, *50*, 2082–2091. [CrossRef] [PubMed]
30. NASA. Surface Meteorology and Solar Energy. 2018. Available online: <https://eosweb.larc.nasa.gov/cgi-bin/sse/sse.cgi?skip@larc.nasa.gov> (accessed on 2 November 2022).
31. Johnson, G.L. *Wind Energy Systems*; Kansas State University: Manhattan, KS, USA, 2006; p. 449.
32. Renewable Resource Atlas. 2020. Available online: <https://rratlas.kacare.gov.sa/RRMMDataPortal/en/MapTool> (accessed on 11 October 2022).
33. General Electric. 2.75–120 Wind Turbine. 2017. Available online: <https://www.gerenewableenergy.com/wind-energy/turbines/275-120> (accessed on 2 November 2022).

34. GE Energy: GE 2.75–120 Data. 2017. Available online: <https://en.wind-turbine-models.com/turbines/983-ge-general-electric-ge-2.75-120#datasheet> (accessed on 2 November 2022).
35. Lazard. *Lazard’s Levelized Cost of Storage Analysis—Version 5.0*; Lazard: Hamilton, Bermuda, 2019; p. 47.
36. Smith, K.; Saxon, A.; Keyser, M.; Lundstrom, B.; Cao, Z.; Roc, A. *Life Prediction Model for Grid-Connected Li-ion Battery Energy Storage System*; National Renewable Energy Laboratory: Golden, CO, USA, 2017.
37. Lazard. *Lazard’s Levelized Cost of Energy Analysis—Version 11.0*; Lazard: Hamilton, Bermuda, 2017; p. 22.
38. U.S. Energy Information Administration (EIA). *Capital Cost and Performance Characteristic Estimates for Utility Scale Electric Power Generating Technologies*; US Energy Information Administration (EIA): Washington, DC, USA, 2020; p. 212.
39. Moss, S.; Godden, P. Aurecon: Cost and Technical Parameters Review 2020. Consultation Report for Australian Energy Market Operator (AEMO). Revision 3. December 2020. Available online: <https://www.aemo.com.au/> (accessed on 2 November 2022).
40. U.S. DOE. Combined Heat and Power Technology Fact Sheet Series Overview of CHP Technologies. November 2017; pp. 1–4. Available online: <https://www.energy.gov/eere/amo/combined-heat-and-power-basics> (accessed on 2 November 2022).
41. Organization of the Petroleum Exporting Countries. *2016 OPEC World Oil Outlook*; Organization of the Petroleum Exporting Countries: Vienna, Austria, October 2016.
42. EIA. *Annual Energy Outlook 2020: Natural Gas Supply, Disposition, and Prices*; US Energy Information Administration (EIA): Washington, DC, USA, 2020.
43. Natural Gas and the Vision 2030. Jadwa Investment. 2016. Available online: http://www.jadwa.com/en/search/index?q=natural+gas&_buffer=true (accessed on 2 November 2022).
44. Annual Energy Outlook 2020: Petroleum and Other Liquids Prices. 2020. Available online: <https://www.eia.gov/outlooks/aeo/data/browser/#/?id=12-AEO2020&cases=ref2020&sourcekey=0> (accessed on 2 November 2022).
45. *Technical Support Document: Social Cost of Carbon, Methane, and Nitrous Oxide*; Interim Estimates under Executive Order 13990; Interagency Working Group on Social Cost of Greenhouse Gases, United States Government: Washington, DC, USA, 2021.
46. Akar, S.; Beiter, P.; Cole, W.; Feldman, D.; Kurup, P.; Lantz, E.; Margolis, R.; Oladosu, D.; Stehly, T.; Rhodes, G.; et al. *2020 Annual Technology Baseline (ATB) Cost and Performance Data for Electricity Generation Technologies*; National Renewable Energy Laboratory: Golden, CO, USA, 2022. Available online: <https://data.nrel.gov/submissions/145> (accessed on 5 November 2022).
47. Schmidt, O.; Hawkes, A.; Gambhir, A.; Staffell, I. The future cost of electrical energy storage based on experience rates. *Nat. Energy* **2017**, *2*, 1–8. [[CrossRef](#)]
48. U.S. Bureau of Labor Statistics. *Inflation & Prices: Consumer Price Index*; U.S. Bureau of Labor Statistics: Washington, DC, USA, 2021. Available online: <https://www.bls.gov/data/#prices> (accessed on 2 November 2022).
49. Ela, E.; Milligan, M.; Kirby, B. *Technical Report, NREL/TP-5500-51978*; National Renewable Energy Laboratory: Golden, CO, USA, 2011. Available online: <http://www.nrel.gov/docs/fy11osti/51978.pdf> (accessed on 2 November 2022).
50. Bhattacharyya, S.C. Review of alternative methodologies for analysing off-grid electricity supply. *Renew. Sustain. Energy Rev.* **2012**, *16*, 677–694. [[CrossRef](#)]
51. Mandelli, S.; Barbieri, J.; Mereu, R.; Colombo, E. Off-grid systems for rural electrification in developing countries: Definitions, classification and a comprehensive literature review. *Renew. Sustain. Energy Rev.* **2016**, *58*, 1621–1646. [[CrossRef](#)]
52. Mahapatra, S.; Dasappa, S. Rural electrification: Optimizing the choice between decentralized renewable energy sources and grid extension. *Energy Sustain. Dev.* **2012**, *16*, 146–154. [[CrossRef](#)]
53. Oparaku, O.U. Rural area power supply in Nigeria: A cost comparison of the photovoltaic, diesel/gasoline generator and grid utility options. *Renew. Energy* **2003**, *28*, 2089–2098. [[CrossRef](#)]
54. Mousavi, S.A.; Zarchi, R.A.; Astaraei, F.R.; Ghasempour, R.; Khaninezhad, F.M. Decision-making between renewable energy configurations and grid extension to simultaneously supply electrical power and fresh water in remote villages for five different climate zones. *J. Clean. Prod.* **2021**, *279*, 123617. [[CrossRef](#)]
55. Nfah, E.M.; Ngundam, J.M. Feasibility of micro-hydro and photovoltaic hybrid power systems for remote villages in Cameroon. *Renew. Energy* **2009**, *34*, 1445–1550. [[CrossRef](#)]
56. Dalton, G.J.; Lockington, D.A.; Baldock, T.E. Feasibility Analysis Of Stand-Alone Renewable Energy Supply Options For A Large Hotel. *Renew. Energy* **2008**, *33*, 1475–1490. [[CrossRef](#)]
57. Bhuiyan, M.M.; Asgar, M.A.; Mazumder, R.K.; Hussain, M. Economic evaluation of a stand-alone residential photovoltaic power system in Bangladesh. *Renew Energy* **2000**, *21*, 403–410. [[CrossRef](#)]
58. Bouffard, F.; Kirschen, D.S. Centralised and distributed electricity systems. *Energy Policy* **2008**, *36*, 4504–4508. [[CrossRef](#)]

Disclaimer/Publisher’s Note: The statements, opinions and data contained in all publications are solely those of the individual author(s) and contributor(s) and not of MDPI and/or the editor(s). MDPI and/or the editor(s) disclaim responsibility for any injury to people or property resulting from any ideas, methods, instructions or products referred to in the content.